Radiative and Nonradiative Excited State Relaxation Channels in Squaric Acid Derivatives Bearing Differently Sized Donor Substituents: A Comparison of Experiment and Theory

Claudia Gude and Wolfgang Rettig*

Institut für Chemie, Physikalische und Theoretische Chemie, Humboldt-Universität zu Berlin, Bunsenstrasse 1, D-10117 Berlin, Germany

Received: January 11, 2000; In Final Form: June 6, 2000

The photophysical properties of squaric acid derivatives bearing two piperidino (SQ-DP) or two indolinylidenemethyl groups (SQ-IN) are determined and compared to the results of ab initio quantum chemical calculations on smaller model systems. In both cases, a temperature-dependent nonradiative decay process is observed which quenches the fluorescence. The latter is especially efficient for SQ-DP, because the radiative transition is forbidden in this case. It is concluded that in both compounds, twisting relaxations are important, leading to a close approach of ground and excited states. For SQ-IN, this relaxation process is connected with an increase of the excited-state dipole moment and explains why the nonradiative losses are enhanced in polar solvents.

Introduction

Squaraine derivatives are popular dyes in the visible region used for photosensitization in imaging processes[1−3] and in solar energy conversion.[4,5] Their photophysics, however, have only recently started to raise interest,[6−18] and most of these studies focus on squaraines bearing anilino donors like SQ-DMA, although a large variety of dyes with quite different donors are available.[19−23] Whereas SQ-DMA is known to exhibit quite strong fluorescence,[9,11,14−16] nothing has been reported about the fluorescence properties of the squaraine compound SQ-DP and little is known[23] about the fluorescence of cyanine-type squaraines like SQ-IN (Scheme 1). On the other hand, there are some reports with respect to the synthesis and absorption data of these compounds in the literature.[23−25] We therefore undertook some systematic photophysical investigations regarding the luminescence properties of these squaraines. In contrast to the relatively high fluorescence quantum yields of SQ-DMA, the values determined for SQ-IN are clearly reduced, and SQ-DP does not show fluorescence at all for room temperature conditions.

In order to understand these differences and in an attempt to elucidate possible excited state relaxation processes, we measured and compared the photophysical properties of these dyes at various temperatures and tried to correlate them with the results of ab initio quantum chemical calculations. Only a few theoretical studies, most of them based on semiempirical methods, have been done until now.[26−28]

A further interesting question is how the excited-state properties of squaraine dyes like SQ-IN relate to those of the corresponding polymethine (cyanine) dyes. Scheme 2 shows a comparison of resonance structures and absorption properties of these two closely related classes of dyes. SQ3 is the shortest prototype dye related to SQ-DP, and the number *n* (SQ*n*,CY*n*) corresponds to the number of carbon p-atoms involved in the cyanine type subunit of the chromophore. It can be seen that the absorption wavelengths of squaraines are approximately equivalent to that of the corresponding cyanines. The differences of squaraine and cyanine structure are mainly characterized through the addition of an oxygen substituent, the bridging of the central carbon atoms by a carbonyl group, and the elimination of the typical cyaninic all-trans skeleton. Thus, squaraines like SQ-IN may be viewed as a special class of polymethine-(cyanine-) like dyes which are nonionic, in contrast to the ionic cyanine dyes. This has some interesting consequences such as increased solubility in weakly polar solvents, the possibility for molecular dipoles, etc.

SCHEME 1: Chemical Structures of Some Squaraine Compounds

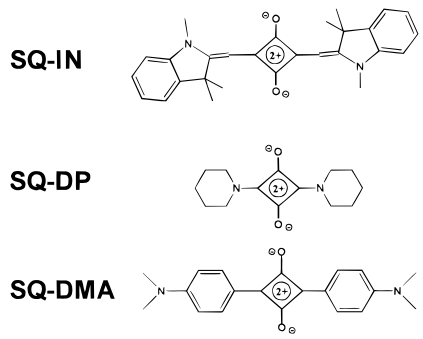

Considering the possible resonance structures of the squaraines, the question arises whether the central four-membered ring can be compared to other ionic cyclobutadiene derivatives. Donor−acceptor substituted cyclobutadienes are known from theoretical studies[10,29,30] to possess excited state relaxational possibilities leading to a sizable energetic approach of S_1 and S_0 or to conical intersections and thus to the possibility for strong fluorescence red shifts and/or excited-state photochemical funnels.[30,31]

Two types of relaxation coordinates are important in this case: The in-plane relaxation of the cyclobutadiene skeleton through bond length changes[10,29] and twisting relaxations of the substituents, leading to biradicaloid states[30] related to the well-known "twisted intramolecular charge transfer" (TICT) states.[32−36]

In addition to the photophysical studies we tried to approach these questions by quantum chemical calculations in view of the unavailability of suitable model compounds.

10.1021/jp000139w CCC: $19.00
Published on Web 08/08/2000

SCHEME 2: Comparison of the Absorption Properties[54,58] of Squaraine and Cyanine Dyes with Carbon Chains of Similar Length

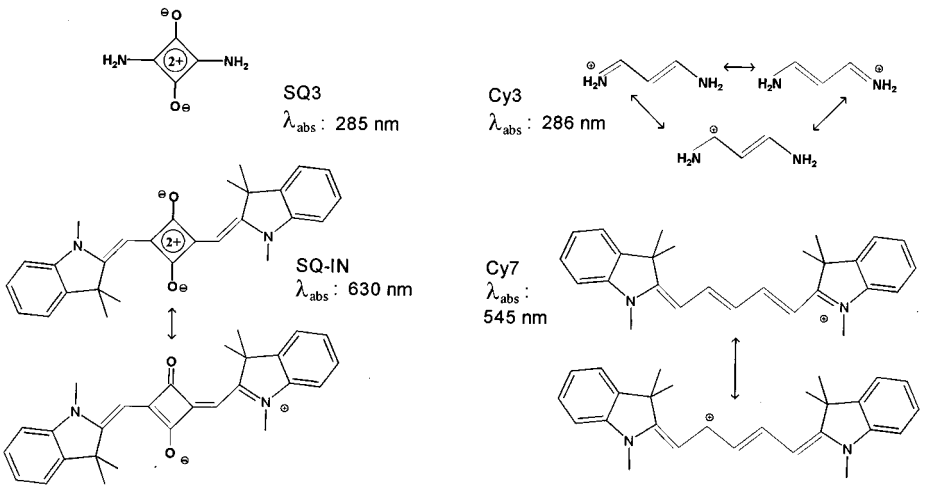

Experimental Details

The preparation of both squaraine compounds SQ-IN and SQ-DP is described in refs 24, 37, and 38. The samples used were a gift of Prof. S. Dähne. The absence of possible traces of impurities was confirmed by high-performance thin-layer chromatography. SQ-DP was further checked by mass spectrometry without an indication of an impurity. The stability with respect to thermal and photoinduced decomposition of the squaraines was also checked. For this purpose, the samples with a given optical density were illuminated under the typical conditions of fluorescence measurements or were stored in a dark room temperature environment for 1 or 2 weeks. After this the optical densities were determined. Absorption spectra were measured on a Shimadzu (UV-210A) spectrometer, and quantum-corrected fluorescence and excitation spectra (concentrations $< 10^{-4}$ M) were determined on a Perkin-Elmer 650-60 fluorimeter. The colorant Basic Blue 3 was used as quantum counter for determination of the correction curve, enabling to measure corrected emission spectra in the range 300−700 nm.[39] For correcting the red tail of the spectra beyond 700 nm, the correction curve was further extended by means of the wavelength characteristics of the photomultiplier. Fluorescence quantum yields were determined relative to an ethanolic solution of Rhodamin 101 ($\Phi_f = 1.0$) and corrected for the refractive index of the solvents. Fluorescence spectra, measured in aerated solutions, were independent of the excitation wavelength. The determination of low-temperature fluorescence quantum yields took into account the temperature dependence of the refractive index as well as the solvent contraction (density increase) with lowering temperature. Fluorescence lifetimes were determined for aerated solutions, using a single photon counting equipment and synchrotron radiation from the Berlin electron storage ring BESSY as excitation source. The experimental setup is described in detail elsewhere.[40] The decay curves were fitted using the iterative reconvolution procedure (Marquardt algorithm), which allowed a time resolution down to 0.1 ns. For SQ-IN, almost all fluorescence decay curves have been determined at least for two different emission wavelengths. The data sets for a given solvent were singly as well as globally analyzed, leading to a higher reliability of the fitted parameters.[41−43] The decay times were treated as linked parameters, and amplitudes and time shift were fitted as free variables. Comparative measurements with polarization filters set to the magic angle position were carried out for SQ-IN. A possible influence of anisotropy effects could thus be excluded. Because of the extremely low intensity of the emission this check could not be performed for SQ-DP.

SCHEME 3: Chemical Structures of the Squaraine Models Used for ab Initio Calculations

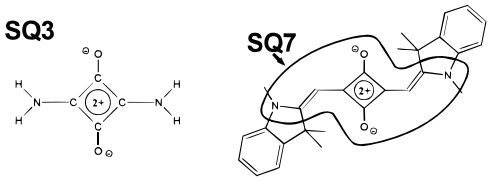

Computational Details

Geometry optimizations were carried out at the restricted Hartree−Fock (RHF) and open shell restricted Hartree−Fock (ORHF) level including analytical gradient techniques. In order to reduce the extent of calculational resources used for the ab initio study, the model compounds SQ3 and SQ7 have been chosen as prototypes for squaraines with alkyl- and aryl side chains (Scheme 3). In both cases, these model compounds correspond to the smallest subunits of the experimental squaraines comprising the essential functional groups.

Pople basis sets 3-21G and 6-31G*[44,45] were used in the major part of the calculations. Furthermore, a double-ζ basis with additional polarization functions (DZP basis)[46,47] was applied in some cases to verify the results obtained using smaller basis sets. Calculations were carried out with regard to geometry optimizations, Mulliken population analysis,[48] and calculation of quadrupole moments as well as energy levels for the ground state and several excited states of the two models SQ3 and SQ7 including configuration interaction (CI).

Single-point CI calculations were performed using a multi-reference direct CI[49] and a conventional MR-SDCI[50] method, the latter being particularly suited for the investigation of excited states of systems of low molecular symmetry.

Using a 6-31G* basis set for SQ3, the molecular basis set consists of 128 atomic orbitals. To restrict the number of generated singly and doubly excited configuration, 15 doubly occupied molecular orbitals were used as a fixed core. For SQ7, a 3-21G basis set corresponding to 124 primitive Gaussians and a core of 30 doubly occupied molecular orbitals was chosen.

Experimental Results

(a) SQ-IN. SQ-IN shows weak to sizable fluorescence, which

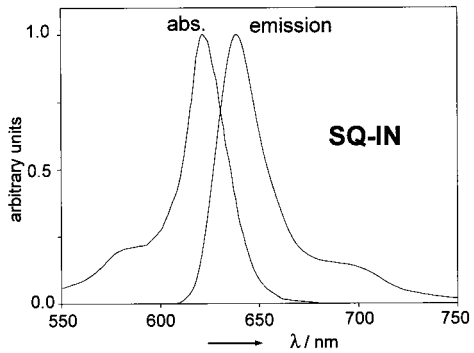

Figure 1. Absorption and fluorescence spectra of SQ-IN in ethanol at room temperature

TABLE 1: Spectral and Photophysical Data for SQ-IN in Solvents of Different Polarity at Room Temperature

solvent	Δf^a	λ_{abs}/nm	λ_{em}/nm	ϕ_f	τ_f/ns
toluene	0.013	638	650	0.378	1.44
1,4-dioxane	0.020	635	646	0.298	1.09
chloroform	0.148	633	644	0.188	1.00
diethyl ether	0.167	628	640	0.219	1.03
ethyl acetate	0.201	631	642	0.185	0.67
tetrahydrofuran	0.210	635	646	0.209	0.83
dichloromethane	0.218	633	644	0.134	0.59[b]
butyronitrile	0.275	632	644	0.127	0.61[b]
ethanol	0.289	628	638	0.083	0.37[b]
acetonitrile	0.305	629	640	0.049	0.16[c]
methanol	0.308	623	636	0.036	<0.1

[a] $\Delta f = (\epsilon - 1)/(2\epsilon + 1) - (n^2 - 1)/(2n^2 + 1)$. [b] Further short-lived component (≈0.1 ns) of smaller weight present. [c] Further minor component (≈0.5 ns) present.

is the mirror image of the absorption (Figure 1) and exhibits a very small Stokes shift in accordance with a previous study[23] on related derivatives of SQ-IN. The red shoulder can be interpreted as a vibronic band, similar to the blue shoulder in the absorption spectrum.

The absorption coefficient $\epsilon(\lambda_{max}$=625 nm) was previously determined as 4.6×10^5 L cm^{-1} mol^{-1} in ethanol.[24] The band half-widths of the spectra of SQ-IN are very narrow (around 600 cm^{-1}), comparable to those of typical cyanine dyes.[51] The fluorescence excitation spectrum closely follows the absorption spectrum, indicating that the fluorescence quantum yield is independent of the excitation wavelength. Thermal and photochemical stability of this dye were tested by monitoring a dilute solution in the dark and under the illumination conditions used to excite the fluorescence spectra and proved to be quite satisfactory. For example, the thermal stability of SQ-IN in EtOH stored in the dark for 1 week was 100%, while illumination of the sample (30 min) led to a small lowering of the optical density by 6%. In solvents more polar than tetrahydrofuran (see Table 1), the fluorescence decay curves had to be fitted by a biexponential function, but the relative weight of the second component was rather small. Repeated measurements indicated that the additional short-lived component is not explainable by the presence of small amounts of photochemical or thermal decomposition products. Variation of the concentration by a factor 25 did not change the values and relative weights of the decay components.

The spectral and photophysical parameters as a function of solvent polarity as measured by the Lippert parameter Δf are collected in Table 1. Both absorption and fluorescence spectra show very small solvent shifts, but the changes of fluorescence quantum yields and lifetimes are strong and indicate a solvent-polarity dependent nonradiative decay process. Employing the

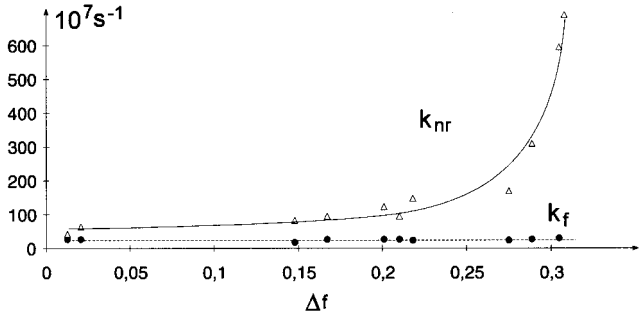

Figure 2. Photophysical rate constants for SQ-IN as a function of solvent polarity parameter Δf at room temperature

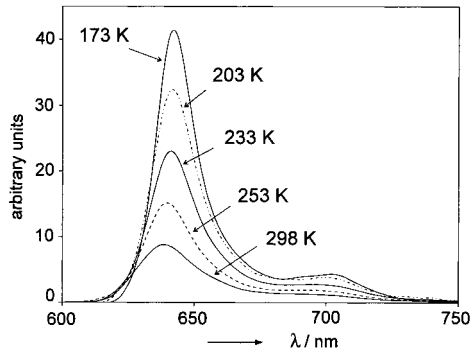

Figure 3. Temperature effect on the fluorescence spectra of SQ-IN in ethanol.

TABLE 2: Photophysical Rate Constants for SQ-IN in Selected Solvents at Room Temperature

solvent	$k_f{}^a/10^7$ s^{-1}	$k_{nr}/10^7$ s^{-1}
chloroform	18.8	81.2
diethyl ether	26.9	95.9
butyronitrile	24.7	169.8
ethanol	27.9	308.2
acetonitrile	30.6	594.3

[a] Mean value of the solvents 25.8 s^{-1}.

usual description of ϕ_f and τ_f by the fluorescence rate constant k_f and the sum of all nonradiative rate constants, k_{nr}^{tot}, (eqs 1, 2), expressions for k_f and k_{nr}^{tot} are readily derived (eqs 3, 4) and applied to the data (Figure 2).

k_f turns out to be approximately solvent independent, but k_{nr}^{tot} clearly increases along with solvent polarity. Values for selected solvents are collected in Table 2.

$$\phi_f = \frac{k_f}{k_f + k_{nr}^{tot}} \quad (1)$$

$$\tau_f = \frac{1}{k_f + k_{nr}^{tot}} \quad (2)$$

$$k_f = \frac{\phi_f}{\tau_f} \quad (3)$$

$$k_{nr}^{tot} = k_f(\phi_f{}^{-1} - 1) \quad (4)$$

Upon cooling the solutions, the fluorescence intensity strongly increases and the spectra show a weak redshift (Figure 3). The increase of the quantum yields is paralleled by lengthened fluorescence lifetimes, and the effect is much stronger in highly polar solvents as compared to weakly polar ones (Table 3). At

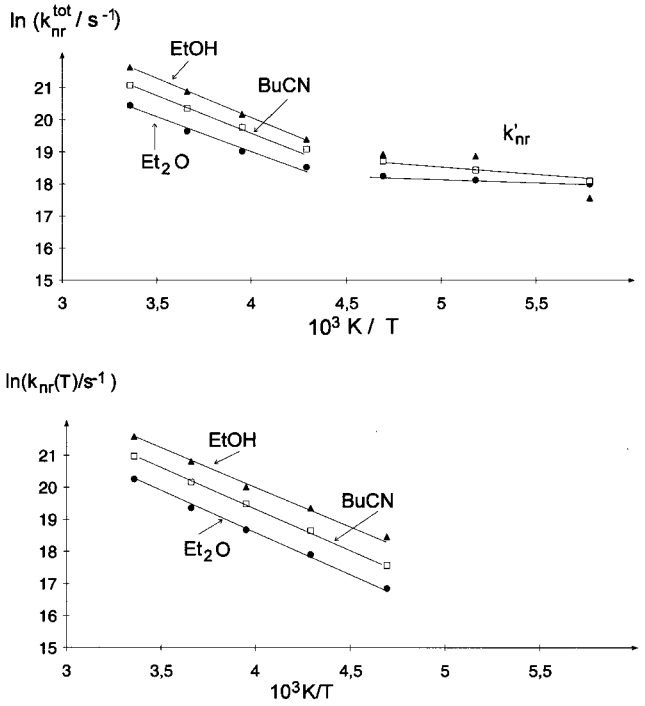

Figure 4. (a) Total nonradiative decay rate constants for SQ-IN in differently polar solvents as a function of temperature, as derived from fluorescence quantum yields (eq 4). (b) temperature-dependent part of k_{nr} as derived from fluorescence lifetimes (eq 5).

TABLE 3: Low Temperature Fluorescence Quantum Yields and Lifetimes of SQ-IN in Solvents of Different Polarity

T/K	Et_2O[a]	BuCN[b]	EtOH[c]	*T*/K	Et_2O[a]	BuCN[b]	EtOH[c]
			ϕ_f as *f*(solvent,*T*)				
298	0.22	0.13	0.08	213	0.77	0.65	0.63
273	0.44	0.25	0.18	193	0.79	0.71	0.63
253	0.61	0.39	0.32	173	0.81	0.79	0.89
233	0.72	0.58	0.55				
			τ_f/ns as *f*(solvent,*T*)				
298	1.03	0.61	0.37	213	2.76	2.61	2.24
273	1.67	1.09	0.69	193	2.86	2.87	2.39
253	2.12	1.59	1.20	173	2.88	2.90	2.61
233	2.49	2.15	1.68	143	2.93		2.85[d]

[a] Diethyl ether. [b] *n*-Butyronitrile. [c] Ethanol. [d] At 113 K.

low temperature, quantum yields and lifetimes converge to a solvent-independent value.

The nonradiative rates as calculated using eq 4 are shown in Figure 4a, and Figure 4b shows the same data evaluated from the fluorescence lifetimes by using eq 5. In this case, only the temperature-dependent part $k_{nr}(T)$ of k_{nr}^{tot} (see eq 6) is recovered. As can be seen from a comparison of Figure 4, a and b, $k_{nr}(T)$ and k_{nr}^{tot} are very similar, indicating that other temperature-independent deactivation channels k'_{nr} (like intersystem crossing and internal conversion) are of minor importance at higher temperatures.

$$k_{nr}(T) = \tau^{-1}(T) - \tau_{ref}{}^{-1} \quad (5)$$

$$k_{nr}^{tot} = k'_{nr} + k_{nr}(T) \quad (6)$$

The activation energies E_a for the process $k_{nr}(T)$ were calculated from the slopes of the Arrhenius plots, Figure 4a,b, and are collected in Table 4 together with the activation energy of viscous flow of the pure solvent, E_η. E_a is sizeably larger than E_η, indicating a process connected with an intrinsic activation barrier.[52] The quenching process can therefore be viewed as an adiabatic photoreaction channel leading to a nonemissive excited-state funnel or conical intersection[30,31,53] after crossing an activation barrier.

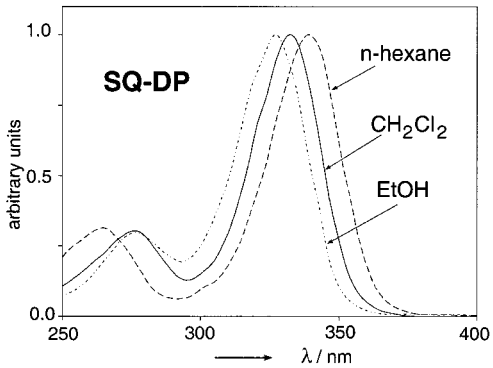

Figure 5. Absorption spectra of SQ-DP in differently polar solvents at room temperature

TABLE 4: Arrhenius Parameters for SQ-IN in Various Solvents, and the Activation Energies of Solvent Viscosity

solvent	ln(A/s^{-1})	E_a/kJ mol $^{-1}$	E_η/kJ mol $^{-1}$
Et_2O	28.6[a] [27.2[b]]	20.7[a] [16.9[b]]	6.8[c]
BuCN	29.5[a] [28.1[b]]	21.1[a] [17.6[b]]	8.8[d]
EtOH	29.3[a] [29.7[b]]	19.3[a] [19.9[b]]	16.6[e]

[a] From Figure 4b (5 values). [b] From Figure 4a (4 values). [c] *Handbook of Chemistry and Physics*, 73rd ed.; CRC Press: Boca Raton, FL, 1992−3. [d] *Databook on Viscosity of Liquids*; Hemisphere Publ. Inc.: New York, 1989. [e] Pantke, E. R.; Labhart, H. *Chem. Phys. Lett.* **1973**, *23*, 479.

(b) SQ-DP. The alkylamino-substituted squaraine compound SQ-DP proved to be totally nonfluorescent at room temperature in ordinary solvents. In contrast to SQ-IN, the long-wavelength absorption band at 340 nm is broadened (half-width 2700 cm^{-1}) and exhibits a sizable negative solvatochromic shift which is not paralleled by the absorption band at around 270 nm (Figure 5). The latter is therefore a separate electronic transition and not a vibronic band. This can also be concluded from measurements of the polarization direction of both transitions by liquid crystal induced circular dichroism (LCICD).[25]

The extinction coefficient for the main absorption band was determined as $\epsilon(\lambda_{max}$=339 nm) = 29 200 L cm^{-1} mol^{-1} in methylcyclohexane.

Upon cooling to 173 K and below, a weak fluorescence consisting of a normal and a strongly red-shifted band around 490 nm could be detected in the nonpolar solvent mixture MCH/IP (methylcyclohexane/isopentane 1:4), but not in ethanol. A rough estimate of the fluorescence quantum yield (173 K: $\phi_f \approx 3 \times 10^{-4}$; 133 K: $\phi_f \approx 6 \times 10^{-3}$; 113 K: $\phi_f \approx 1 \times 10^{-2}$) indicates its strong increase (factor ≈ 30) with lowering of the temperature (Figure 6). In order to be certain about this weak fluorescence, we tested SQ-DP by chromatography and mass spectrometry, without indication of an impurity. A further purification step (sublimation) also led to the same spectral results. In view of the fluorescence excitation spectrum (Figure 6) which is not identical to but resembles the absorption spectrum at room temperature with bands at similar position we conclude that the absorbing and emitting species is indeed SQ-DP, and that the large Stokes shift of the 490 nm band indicates a relaxation process prior to emission. Its fluorescence intensity increases with decreasing temperature indicating a viscosity- or temperature-controlled nonradiative process which occurs after the initial relaxation process which causes the

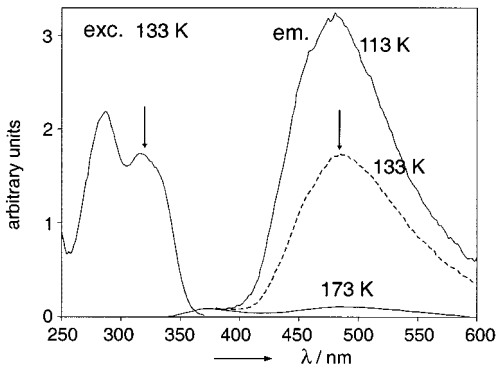

Figure 6. Fluorescence and fluorescence excitation spectra of SQ-DP in MCH/IP (1:4) at low temperature. The excitation and observation wavelength are indicated by the arrows.

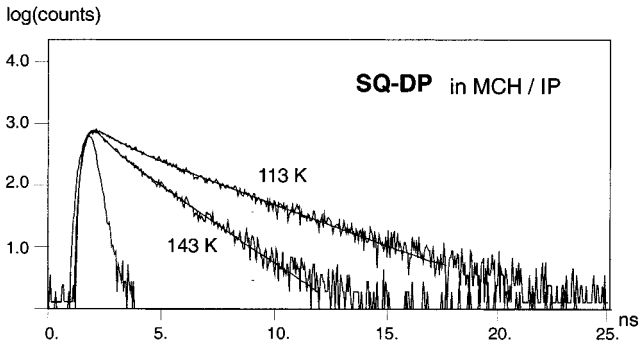

Figure 7. Fluorescence decay traces of SQ-DP in MCH/IP (1:4) at low temperatures. The excitation profile of BESSY synchrotron radiation is also shown.

TABLE 5: Main Fluorescence Decay Times Determined for SQ-DP in MCH/IP[a]

T/K	143	133	113	77
τ_f/ns[b,d]	1.6	2.4[c]	3.0	4.2

[a] Methylcyclohexane/isopentane (1:4). [b] $\lambda_{exc} = 320-330$ nm, $\lambda_{em} = 480$ nm. [c] Identical results for 320 and 288 nm excitation. [d] A second shorter component (relative weight ≈ 20%) ranging between 0.5 and 1.4 ns was also present.

unusually large Stokes shift (≈9900 cm^{-1}) observed in a nonpolar low-temperature solvent.

This view is confirmed by the fluorescence lifetime results (Figure 7 and Table 5) which are complicated (biexponential behavior) but show a clear tendency for lifetime shortening with increasing temperature.

Using the approximate fluorescence quantum yield given above for 113 K, we determine a radiative rate constant $k_f = 3.3 \times 10^6\ s^{-1}$, indicating that the emission process is strongly forbidden for SQ-DP, in contrast to the allowed fluorescence observed for SQ-IN ($k_f = 2.6 \times 10^8$). A similarly strong difference is observable when the nonradiative rate constants are compared: the value for SQ-DP ($k_{nr} = 150 \times 10^8\ s^{-1}$ in MCH at 173 K) is much larger than that for SQ-IN ($k_{nr} = 0.4 \times 10^8\ s^{-1}$ in EtOH at 173 K).

Computational Results

(a) SQ3 as model for SQ-DP. The optimization of the ground state (3-21G/RHF) of SQ3 leads to a symmetric geometry (D_{2h}) with a good agreement between calculated and experimental bond parameters for SQ-DP.[27] On the basis of this geometry the energies of various electronic transitions have been determined by 3-21G/MRD-CI calculations and complemented by (6-31G*/DZP) Direct CI (Table 6).

TABLE 6: Calculation (6-31G*/Direct CI) of the Transition Energies (in eV) and Characteristics Refering to the Optimized Ground State Energy of SQ3

transition		ΔE^a/eV	ΔE^b/nm	character of transition
$S_0 \rightarrow S_1$	$^1A_g \rightarrow {}^1B_{1g}$	4.23	293	$n \rightarrow \pi^{*c}$
$S_0 \rightarrow S_2$	$^1A_g \rightarrow {}^1B_{1u}$	4.53	274	$\pi \rightarrow \pi^*$
$S_0 \rightarrow S_3$	$^1A_g \rightarrow {}^1B_{2g}$	5.21	238	$n \rightarrow \pi^{*c}$
$S_0 \rightarrow S_4$	$^1A_g \rightarrow {}^1B_{3u}$	5.44	228	$n \rightarrow \pi^*$
$S_0 \rightarrow S_5$	$^1A_g \rightarrow {}^1B_{2u}$	6.67	185	$\pi \rightarrow \pi^*$
$S_0 \rightarrow T_1$	$^1A_g \rightarrow {}^3B_{1u}$	2.74	453	$\pi \rightarrow \pi^*$
$S_0 \rightarrow T_2$	$^1A_g \rightarrow {}^3B_{1g}$	4.20	295	$n \rightarrow \pi^{*c}$

[a] Referring to the ground state energy: $E(S_0) = -412.959497$ au. [b] Calculated absorption wavelength. [c] Symmetry-forbidden transition.

TABLE 7: Calculation (6-31G*/HF) of the Quadrupole Moment *Q* for the Ground State and the Optically Allowed Singlet Excited States of SQ3

state	$1^1A_g(S_0)$	$1^1B_{1u}(S_2)$	$1^1B_{3u}(S_4)$	$1^1B_{2u}(S_5)$
$Q/10^{-26}$ esu	66.2	45.1	37.7	79.6

SCHEME 4: Planar and Twisted Conformations as Possible Excited State Relaxation Pathways of SQ3

Pathway (i)	$\vartheta_1 = 0° / \vartheta_2 = 0°$	D_{2h}
Pathway (ii)	$\vartheta_1 = 0° / \vartheta_2 = 90°$	C_{2v}
Pathway (iii)	$\vartheta_1 = 90° / \vartheta_2 = 90°$	D_{2h}

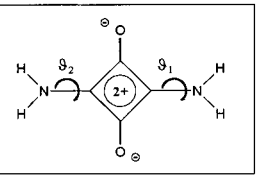

The comparison of these calculations shows that the choice of basis set has neither influence on the energetic following of states nor on the character of states. According to the calculations, the lowest excited state (S_1) is of symmetry-forbidden character, and the first absorption band should correspond to the $S_0 \rightarrow S_1$ transition. The calculated transition energy indeed exhibits a satisfactory agreement with the absorption spectrum of SQ3 in KBr and H_2SO_4, which possesses maxima at 293 nm (4.23 eV) and 285 nm (4.35 eV).[54]

An analysis of the wave functions was carried out and the state character was classified either as $\pi \rightarrow \pi^*$ or as $n \rightarrow \pi^*$ as indicated in Table 6. The analysis of the ground and excited state wave functions reveals that the corresponding states are well represented by one single leading configuration ($C_{CI} > 85\%$). Therefore, the investigation of the electronic distribution by a Mulliken population analysis is justified.

In general, the excitation of SQ3 leads to an electron flow (for both $\pi \rightarrow \pi^*$ or $n \rightarrow \pi^*$ type of state) from the carbonyl subunit to the central part of the molecule. Because of its inversional symmetry, SQ3 has a vanishing dipole moment. The observed solvent polarity dependence of the absorption wavelength is therefore caused by other than dipolar mechanisms. Apart from direct solute−solvent interaction such as aggregate formation, quadrupole stabilization effects can be considered.[55] The calculated quadrupole moments are given in Table 7.

The quadrupole moment of the first allowed excited state (S_2) is smaller than that of the ground state, $Q(1^1A_g) > Q(1^1B_{1u})$. This can explain the observed hypsochromic shift of the long wavelength band with increasing solvent polarity (Table 1).

In the search for a mechanism explaining the occurrence of the strong nonradiative deactivation process, which was experimentally observed for SQ-DP, various possible excited state relaxation pathways (Scheme 4) were examined for SQ3. For the different pathways, the relaxation was restricted to (i) the planar geometry, allowing bond length changes analogous to the in-plane relaxation of push−pull cyclobutadienes,[29,30,56] (ii)

TABLE 8: CI Calculation (6-31G*/Direct CI) of the Transition Energies, ΔE_{rel}[a]/kJ mol^{-1}, of SQ3 Assuming a Planar Relaxation Scheme 4(i) (Optimized $S_0(A_g)$, $S_1(B_{1g})$, and $S_2(B_{1u})$ Geometries) or a Doubly Twisted SQ3 Conformation Scheme 4(iii) (Optimized $S_1(B_{1g})$ Geometry)

	planar relaxation pathway (i)			doubly twisted conformer pathway (iii)
state	$S_0(A_g)$-optimized geometry	$S_1(B_{1g})$-optimized geometry	$S_2(B_{1u})$-optimized geometry	$S_1(B_{1g})$-optimized geometry
S_0 $1A_g$	0.0	32.2	33.9	238.5
S_1 $1B_{1g}$	407.5	359.8	369.4	340.5
S_2 $1B_{1u}$	437.2	391.6	380.7	525.1

[a] Referring to the ground state energy: $E(S_0) = -412.959497$ au.

a single twisted amino group, and (iii) a doubly twisted rotamer as indicated in Scheme 4.

The geometries in the S_1 and S_2 excited states were optimized for the planar molecule (3-21G/ ROHF) and taken as basis for subsequent CI calculations. It was found that bond length alone result in only small effects on the S_0/S_1 energy gap (Table 8), which stays large. Hence pathway (i) cannot be responsible for the rapid nonemissive deactivation of the excited system but probably for part of the large Stokes shift observed. The twisting pathways (ii) and (iii) of Scheme 4, however, lead to a significant approach of S_0 and S_1. On the basis of the ground state geometries of both rotamers the transition energies were calculated (3-21G/MRD-CI). The following trend was found: with increasing twisting process the energy of the $S_1(1^1B_{1g})$ state is lowered, whereas the S_0 state becomes strongly destabilized. A strongly reduced S_0/S_1 energy gap of around 15 kJ/ mol was found for the doubly twisted molecule of conformation (iii). Some reduction of the energy gap was also indicated by the calculations on conformation (ii).

Additional ab initio calculations on a higher level of accuracy (6-31G*/direct CI) (see Table 8) and with geometry optimization of the $S_1(1^1B_{1g})$ excited molecule, however, lead to a somewhat larger energy difference of S_0/S_1 state. These model calculations, which are of more qualitative character, lead to the suggestion of the excited state relaxation process producing the quenching in SQ-DP.

The comparison of π-charge distribution indicates that charge transfer is of minor importance and does not accompany the twisting relaxation as it is in the case of TICT compounds.[32−36]

(b) SQ7 as Model for SQ-IN. SQ7 serves as computational model compound for the discussion of the photophysical properties of SQ-IN (Scheme 3). The ground state optimization results for SQ7, conducted with both C_{2v} and C_{2h} symmetry restriction, show a good agreement with bond length data for SQ-IN.[57] A geometric structure of C_{2h} symmetry (the conformation depicted in Scheme 3) is energetically favored. The transition energies to the first excited states were calculated (3-21G/MRD-CI) on the basis of the optimized ground state geometry. In contrast to SQ3, the first excited state was found to be optically allowed, consistent with the large value of the fluorescence rate constant k_f determined for SQ-IN (Table 2). The comparison of a Mulliken population analysis (6-31G*) for the ground and the first excited state indicates a shift of electron density within the polymethine type side chain and a decrease in charge density around the carbonyl oxygen.

A close relationship of squaraines with cyanines has been discussed.[26,58] It can therefore be expected that a process similar to the cis−trans isomerization of the cyanines should also be of importance for the squaraine derivatives like SQ-IN. Therefore, qualitative calculations testing the influence of rotational motion were carried out taking into account different possibilities of bond twisting (Scheme 5).

SCHEME 5: Possible Bond Twisted Structures of SQ7

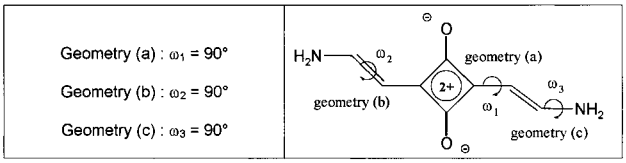

TABLE 9: CI Calculation (3-21G/ MRDCI) of the Ground and Excited State Energies, ΔE[a]/kJ mol^{-1}, for the Planar and Several Conformations of SQ7 with One Twisted Bond ($\omega = 90°$). for Definition of the Geometries of Types a, b, and c (See Scheme 5)

		single twisted bond		
state	planar geometry	geometry a	geometry b	geometry c
S_0	0.0	62.3	170.3	54.0
S_1	243.9	260.2	202.5	289.1
S_2	260.7	323.0	472.8	318.4
$\Delta E(S_1 \rightarrow S_0)$	243.9	197.9	32.2	235.1

[a] Energy with respect to the ground state of the planar conformer $E(S_0) = -563.153687$ au.

When comparing the theoretical results of the model compound SQ7 with those of the experiments, it has to be kept in mind that different experimental molecules can possess a limited rotational freedom, e.g., for SQ-IN, a rotation process of type c is excluded, whereas for SQ-DMA exclusively bond twisting of type a can occur. The ab initio calculations reveal further that symmetrically doubly twisted conformations are strongly destabilized for both ground and excited states of SQ7. This finding is in contrast to SQ3 where the energy of the first excited state was lowered by a symmetrical double twist.

As can be seen from Table 9, geometries a and c are energetically disfavored, whereas the bond twisting of type b leads to a significant stabilization of the first excited state. In the latter case, a very small energy gap $\Delta E(S_0/S_1)$ results from a simultaneous strong destabilization of the ground state. The dipole moment of the S_1 excited geometry b was calculated as 6.0 D, while the planar system possesses a vanishing dipole moment, due to its inversional symmetry. We tentatively conclude from these calculations that a possible nonradiative channel with narrow S_1/S_0 gap, probably situated in the neighborhood of a conical intersection,[59] is connected with the twisting of the double bond (geometry b) and with the generation of a highly dipolar excited species.

Discussion

Many of the experimental findings observed for SQ-DP and SQ-IN can be understood with the help of the theoretical results.

(a) SQ-DP. The absorption spectra of SQ-DP can be analyzed by the comparison with the ab initio results for the SQ3 model system. An interpretation, where the optically allowed transitions are assigned to the $S_0(1^1A_g) \rightarrow S_2(1^1B_{1u})$ and $S_0(1^1A_g) \rightarrow S_5(1^1B_{2u})$ fits well with the experimentally observed spectral

TABLE 10: Solvatochromic Effect Resulting from Different Quadrupole Stabilization

transition	quadrupole moment relation	expected solvent shift
$^1A_g \rightarrow {}^1B_{1u}$	$Q(^1A_g) > Q(^1B_{1u})$	blue shift of absorption
$^1A_g \rightarrow {}^1B_{2u}$	$Q(^1A_g) < Q(^1B_{2u})$	red shift of absorption

features of SQ-DP with allowance for a red shift due to the alkyl groups in the experimental molecule (Figure 5). The direction of the transition moment has been experimentally determined along the long molecular axis of SQ-DP[25] consistent with the calculated long wavelength $S_0 \rightarrow S_2$ transition of SQ3. The hypsochromic behavior observed for the first absorption band is explainable by the stabilization of the stronger quadrupole moment of the ground state as compared to the excited state (Table 7) in a polar molecular environment. For the second transition ($S_0 \rightarrow S_5$), a slightly bathochromic behavior is predicted on the basis of the quadrupole moments (Table 10) consistent with the absorption data.

The extremely low fluorescence intensity found for this system can be understood by the calculated strongly forbidden character of the $S_1 \rightarrow S_0(1^1B_{1g} \rightarrow 1^1A_g)$ transition. Therefore, nonradiative relaxation processes can efficiently compete with emission. A possible strong nonradiative relaxation channel is suggested on the basis of calculations of Table 8, connected with a rotational motion of the amino groups. This model is further supported by the increase of fluorescence intensity at low temperatures and sufficiently high solvent viscosity. An estimation of the radiative rate constant $k_f \approx 3.3 \times 10^6\ s^{-1}$ at 113 K confirms the strongly forbidden character of the emission. This unusually low k_f value points to an $n \rightarrow \pi^*$ ("ketone-like") emission. The observed large Stokes shift and a further red shift of the fluorescence with increasing temperature is assumed to result on one hand from the fact that the longest wavelength absorption band corresponds to S_2, but the emission is from S_1 and on the other hand from possible bond relaxation processes maintaining the planarity of the system.

(b) SQ-IN. The spectroscopic behavior of SQ-IN, which possesses an intense long-wavelength transition, differs drastically from that of SQ-DP. The differences are essentially caused by the expanded size of the π-system leading to an energy lowering of $\pi \rightarrow \pi^*$ type transitions. For larger π-systems, the $n \rightarrow \pi^*$ transition is energetically disfavored with respect to the transitions of $\pi \rightarrow \pi^*$ type, and the oscillator strength is generally increased. The intramolecular fluorescence quenching process which was observed for SQ-IN becomes more pronounced with increasing solvent polarity. This can be termed a positive solvatokinetic behavior[35,59,60] and suggests that the activation barrier for this nonradiative process is lowered in more polar solvents, hence that the transition state is stabilized more strongly than the reactant. This fact points to the involvement of charge separation (increase of dipole or quadrupole moments) for the transition state. If the transition state already partially reflects the properties of the final product (or better quenching state/nonradiative excited-state funnel), we can conclude that the funnel or conical intersection has to possess a highly dipolar or quadrupolar nature.

Qualitative ab initio calculations suggest that a bond twisting process of type b (Scheme 5, Table 9) is the favored downhill relaxation process in the first excited state. In addition, a small S_0/S_1 energy difference as well as a relatively large S_1 excited state dipole moment are connected with this twisted geometry. A further indication for the existence of a nonradiative deactivation process connected with bond twisting is given by the fact that SQ-DMA, for which bond twisting of this type is not possible due to molecular bridging, does not exhibit this strong fluorescence quenching.

Further support for the importance of bond-twisting processes for fluorescence quenching processes can be found in studies of squaraines in polymers or in β-cyclodextrin solutions.[6,7] In these studies, a stronger fluorescence was detected when the molecule was confined close to planarity by specific solvent interaction (hydrogen bonding). Investigations of substituent effects (side chain variation) revealed an effective fluorescence quenching for substituents inducing a deviation from planarity. The fluorescence enhancement and lifetime lengthening upon binding SQ-IN derivatives to bovine serum albumin[23] can be understood on the same basis.

Conclusion

The squaraine derivatives SQ-IN and SQ-DP exhibit strongly different photophysical features. This different behavior was also analyzed by quantum mechanical calculations of more simplified model structures. In spite of the general similarity, the ab initio results show that the squaraines studied cannot directly be compared with push−pull cyclobutadienes[29,30,56] or cyanines.[26,58]

It was further found that the size of the π-systems play a significant role for the state ordering of (π,π^*) versus (n,π^*) excited states, which determine the photophysical and photochemical properties of squaraines.

For SQ3, the model structure for SQ-DP, the first excited state is of (n,π^*) character, a finding which is in a good agreement with the weak, largely Stokes shifted emission observed for SQ-DP (resulting from $S_0 \rightarrow S_2$ absorption, subsequent internal conversion $S_2 \rightarrow S_1$ and $S_1 \rightarrow S_0$ emission). Because of the forbidden character of the $S_1 \rightarrow S_0$ radiative transition, a nonradiative return to the ground state can compete efficiently. We suggest, based on the computational results, that bond twisting leads toward a region involving a photochemical funnel (conical intersection), leading to an effective nonemissive excited state deactivation. The most probable twisting process involves both amino groups.

For SQ7 as model for SQ-IN, the first excited state possesses (π,π^*) character corresponding to an optically allowed transition. This is consistent with the relatively strong fluorescence observed for SQ-IN in contrast to that of SQ-DP. Nevertheless, an intramolecular fluorescence quenching process is made evident which increases with solvent polarity. Ab initio calculations of different relaxation pathways reveal that single bond twisting leads to a highly polar S_1 state connected with a lowered energy and strongly decreased S_0/S_1 gap. This type of twisting relaxation could account for the experimentally observed nonradiative relaxation.

Acknowledgment. We thank Prof. S. Dähne for the gift of the squaraine compounds. The support by the Deutsche Forschungsgemeinschaft (SFB 337) and the Bundesministerium für Forschung und Technologie (project 05 5KT FAB9) is gratefully acknowledged. The computational support of and fruitful discussions with V. Bonacic-Koutecký are gratefully acknowledged.

References and Notes

(1) Law, K. Y. *Chem. Rev.* **1993**, *93*, 449.
(2) Law, K. Y. *J. Imaging Sci.* **1987**, *31*, 83.
(3) Tam, A. C.; Balanson, R. D. *IBM J. Res. Dev.* **1982**, *26*, 186.
(4) Piechowski, A. P.; Bird, G. R.; Morel, D. L.; Stogryn, E. L. *J. Phys. Chem.* **1984**, *88*, 934.
(5) Loufty, R. O.; Hsiao, C. K.; Kazmeier, P. M. *Photogr. Sci. Eng.* **1983**, *27*, 5.

(6) Das, S.; Kamat, P. V.; De la Barre, B.; Thomas, K. G.; Ajayagosh, A.; George, M. V. *J. Phys. Chem*. **1992**, *96*, 10327.
(7) Das, S.; Thomas, K. G.; George, M. V.; Kamat, P. V. *J. Chem. Soc., Faraday Trans*. **1992**, *88*, 3419.
(8) Buncel, E.; MCKerrow, A. J.; Kazmaier, P. M. *J. Chem. Soc., Chem. Commun.* **1992**, 1242.
(9) Ferreira, L. F. V.; Costa, S. M. B.; Peireira, E. J. *J. Photochem. Photobiol. A: Chem*. **1991**, *55*, 361.
(10) Michl, J.; Bonacic-Koutecký, V. *Tetrahedron* **1984**, *44*, 7559.
(11) Kamat, P. V.; Das, S.; Thomas, K. G.; George, M. V. *J. Phys. Chem*. **1992**, *96*, 195.
(12) Kamat, P. V.; Das, S.; Thomas, K. G.; George, M. V. *Chem. Phys. Lett*. **1991**, *178*, 75.
(13) Patrick, B.; George, M. V.; Kamat, P. V.; Das S.; Thomas, K. G. *J. Chem. Soc., Faraday Trans.* **1992**, *88*, 3419.
(14) Law, K. Y. *J. Phys. Chem*. **1987**, *91*, 5184.
(15) Law, K. Y. In *Photophysics of Polymers*; Hoyle, C. E., Torkelson, J. M., Eds.; ACS Symposium Series 358; American Chemical Society: Washington, DC, 1987; p 148.
(16) Cornelissen-Gude, C.; Rettig, W.; Lapouyade, R. *J. Phys. Chem. A* **1997**, *101*, 9673.
(17) Rehák, V.; Israel, G. *Chem. Phys. Lett*. **1986**, *123*, 236.
(18) Kazmaier, P. M.; Hamer, G. K.; Burt, R. A. *Can. J. Chem.* **1990**, *68*, 530.
(19) Schmidt, A. H. In *Oxocarbons*; West, R., Ed.; Academic Press: New York, 1980; p 185.
(20) Sprenger, H. E.; Ziegenbein, W. *Angew. Chem*. **1966**, *5*, 894.
(21) Sprenger, H. E.; Ziegenbein, W *Angew. Chem*. **1967**, *6*, 553 and **1968**, *7*, 541.
(22) Fabian, J.; Hartmann, H. *Theor. Chim. Acta (Berl.)* **1975**, *36*, 351.
(23) Terpetschnig, E.; Szmacinski, H.; Lakowicz, J. R. *Anal. Chim. Acta* **1993**, *282*, 633.
(24) Treibs, A.; Jacob, K. *Liebig Ann. Chem*. **1966**, *153*, 699.
(25) Falk, H.; Hofer, O.; Leodolter, A. *Monatsh. Chem*. **1975**, *106*, 983.
(26) Bigelow, W.; Freund, H. J. *Chem. Phys.* **1986**, *107*, 159.
(27) Budzelaar, P. H. M.; Dietrich, H.; Macheleid, J.; Weiss, R.; von Ragué Schleyer, P. *Chem. Ber*. **1985**, *118*, 2118.
(28) Fabian, J.; Mehlhorn, A.; Fratev, F. *Int. J. Quantum Chem*. **1980**, *17*, 235.
(29) Bonacic-Koutecký, V.; Schöffel, K.; Michl, J. *J. Am. Chem. Soc*. **1989**, *111*, 140.
(30) Michl, J.; Bonacic-Koutecký, V. *Electronic Aspects of Organic Photochemistry*; J. Wiley & Sons: New York, 1990.
(31) Bernardi, F.; Olivucci, M.; Robb, M. A. *Chem. Soc. Rev.* **1996**, *25*, 1321. Bernardi, F.; Olivucci, M.; Robb, M. A. *J. Photochem. Photobiol. A: Chem.* **1997**, *105*, 365. Garavelli, M.; Vreven, T.; Celani, P.; Bernardi, F.; Robb, M. A.; Olivucci, M. *J. Am. Chem. Soc.* **1998**, *120*, 1285.
(32) Grabowski, Z. R.; Rotkiewicz, K.; Siemiarczuk, A.; Cowley, D. J.; Baumann, W. *Nouv. J. Chim*. **1979**, *3*, 443.
(33) Rettig, W. *Angew. Chem., Int. Ed. Engl*. **1986**, *25*, 971.
(34) Lippert, E.; Rettig, W.; Bonacic-Koutecký, V.; Heisel, F.; Miehé, J. A. *Adv. Chem. Phys.* **1987**, *68*, 1.
(35) Rettig, W. In *Electron Transfer I*; Mattay, J., Ed.; Topics in Current Chemistry, Vol. 169; Springer-Verlag: Berlin, 1994; p 253.
(36) Rettig, W.; Maus, M. Conformational Changes Accompanying Intramolecular Excited-State Electron Transfer. In *Conformational Analysis of Molecules in Excited States*; Waluk, J., Ed.; Methods in Stereochemical Analysis Series; Wiley-VCH: New York, 2000.
(37) Gauger, J.; Manecke, G. *Chem. Ber*. **1970**, *103*, 3553.
(38) Treibs, A.; Jacob, K. *Angew. Chem*. **1967**, *79*, 581.
(39) Kopf, U.; Heinze, J. *Anal. Chem*. **1984**, *56*, 1931.
(40) Vogel, M.; Rettig, W. *Ber. Bunsen-Ges. Phys. Chem*. **1987**, *91*, 1241.
(41) Globals Unlimited, *User Manual*, Rev. 3; Laboratory for Fluorescence Dynamics, Department of Physics, University of Illinois at Urbana−Champaign 1110 W Green Street, Urbana, IL 61801, June 1990.
(42) Löfroth, J. E. *J. Phys. Chem*. **1986**, *90*, 1160.
(43) Andriessen, R.; Boens, N.; Ameloot, M.; De Schryver, F. C. *J. Phys. Chem*. **1991**, *95*, 2047.
(44) Hehre, W. J.; Radom, L.; Rague-Schleyer, P.; Pople, J. A. *Ab Initio Molecular Orbital Theory*; John Wiley & Sons Inc.: New York, 1986; p 65.
(45) Ditchfield, R.; Hehre, W. J.; Pople, J. A. *J. Chem. Phys*. **1971**, *54*, 724.
(46) Dunning, T. H.; Hay, P. J.; Schaefer, H. F. *Methods of Electronic Structure Theory*; Plenum Press: New York, 1977; p 1.
(47) Huzinaga, S. *J. Chem. Phys*. **1965**, *42*, 1293.
(48) Lowe, J. P. *Quantum Chemistry*; Academic Press Inc.: New York, 1993; p 336.
(49) Roos, B. O.; Siegbahn, P. E. M. edt. Schaefer, H. F. *Methods of Electronic Structure Theory*; Plenum Press: New York, 1977; p 277.
(50) Buenker, R. J. *Studies in Physics and theoretical chemistry*; Current Aspects of Quantum Chemistry 1981; Elsevier: Amsterdam, 1982; p 17.
(51) Javelink, P.; Scaffardi, L. B.; Duchowicz, R. *J. Phys. Chem*. **1996**, *100*, 11630.
(52) Rettig, W.; Fritz, R.; Braun, D. *J. Phys. Chem. A* **1997**, *101*, 6830.
(53) Olivucci, M.; Robb, M. A.; Bernardi, F. Calculations of excited state conformational properties. In *Conformational Analysis of Molecules in Excited States*; Waluk, J., Ed.; Wiley-VCH: New York, 2000; p 257.
(54) Neuse, E. W.; Green, B. R. *J. Am. Chem. Soc*. **1975**, *97*, 3987.
(55) Dähne, S.; Paul, H. *Chem. Ber*. **1964**, *97*, 1625.
(56) Bonacic-Koutecký, V.; Koutecký, J.; Michl, J. *Angew. Chem*. **1987**, *99*, 216.
(57) Kobayashi, Y.; Goto, M.; Kurahashi, M. *Bull. Chem. Soc. Jpn*. **1986**, *59*, 311.
(58) Fabian, J.; Hartmann, H. *Lone ight Absorption of organic Colorants*; Springer Verlag: Berlin, 1980; p 163.
(59) Rettig, W. *Ber. Bunsen-Ges. Phys. Chem*. **1991**, *95*, 259.
(60) Rettig, W.; Majenz, W.; Herter, R.; Létard J. F.; Lapouyade, R. *Pure Appl. Chem.* **1993**, *65*, 1699.